Research Gate: Pharmaceutical Sciences, 15 (3) (2026) 45-54
ISSN – 2319-6831 (0nline)

Research Gate: Pharmaceutical Sciences
www.iresearchonline.com

# Formulation and Evaluation of Demeclocycline Hydrochloride-Loaded Liposomal Transdermal Patch: A Factorial Design Optimization Approach

V. Kavin * and Dr. A. G. Hariharan

*K.M. College of Pharmacy, The Tamil Nadu Dr. M.G.R. Medical University, Chennai, Tamil Nadu, India.*

**ARTICLE INFO**

***Keywords:***
Demeclocycline HCl,
Liposomal vesicles,
Transdermal patch,
Thin-film hydration,
$3^2$ factorial design,
*Ex-vivo* skin permeation

***Article History:***
*Received : 18th September 2026*
*Accepted : 21st September 2026*
*Available online : 21st September 2026*

**ABSTRACT**

Repeated oral dosing of tetracycline antibiotics such as demeclocycline hydrochloride is associated with fluctuating plasma concentrations, gastrointestinal disturbance, and reduced patient adherence, all of which weaken the practical value of the conventional tablet form. Delivering the same drug through the skin sidesteps first-pass metabolism and dosing frequency, provided the molecule can be pushed across the stratum corneum in sufficient quantity, which is where a carrier-assisted approach becomes useful. In the present investigation, demeclocycline HCl was entrapped within phosphatidylcholine–cholesterol vesicles produced by thin-film hydration, and the resulting liposomal dispersion was cast into an HPMC K100/PVA polymer matrix to yield a transdermal patch. A $3^2$ full factorial design (nine runs, F1–F9) was applied to examine how phosphatidylcholine (X1), cholesterol (X2) and HPMC K100 (X3) jointly govern entrapment efficiency, cumulative in-vitro release and folding endurance. Preliminary characterisation — physical description, melting-point analysis, UV scanning and solubility testing — verified the identity and pharmacopoeial-grade purity of the drug sample prior to formulation. Spectral (FTIR) and thermal (DSC) data pointed to the absence of any appreciable drug–excipient incompatibility, while SEM imaging was used to inspect surface texture. Among the nine trial batches, F7 (250 mg phosphatidylcholine : 30 mg cholesterol : 1200 mg HPMC K100) returned the most favourable combination of responses — 87.2 ± 0.4% entrapment, 91.3 ± 0.5% drug release and a folding endurance of 272 ± 3 — and was therefore taken forward for ex-vivo and microbiological testing. Permeation across excised goat skin mounted on a Franz diffusion cell produced a gradual, near-linear release curve that reached roughly 96% cumulative permeation by the tenth hour, without an early burst. Agar-well diffusion assays further confirmed that the drug retained concentration-dependent antibacterial action against E. coli and two S. aureus biotypes, while the solvent-only control produced no zone of inhibition. Collectively, the data indicate that combining liposomal entrapment with a polymeric patch matrix is a practicable route to sustained, skin-mediated delivery of demeclocycline HCl, and that the formulation is a reasonable candidate for subsequent in-vivo evaluation.

## Introduction

The oral route remains the default for most pharmaceutical products, largely because it is inexpensive and easy for patients to use without assistance, yet it carries well-documented drawbacks. A twice- or thrice-daily dosing schedule is often needed to sustain a therapeutic drug level, which burdens the patient and is a recognised driver of poor adherence, and each dose produces a peak-and-trough plasma profile rather than a steady concentration [1,9]. Hepatic first-pass metabolism further reduces the fraction of an oral dose that ever reaches systemic circulation intact, which is particularly relevant for drugs that are extensively metabolised on first passage through the liver [7,8]. Delivering a drug across the skin avoids the gut and the liver altogether: the drug is absorbed directly into the dermal microcirculation, and, because the delivery system rather than digestion controls the rate of input, plasma levels can in principle be held closer to steady state over an extended period [8,22]. The chief obstacle to this route is not the drug but the skin itself: the stratum corneum is a dense, lipid-rich barrier that most molecules cross only slowly, and formulation scientists have spent several decades looking for ways to move more drug across it without damaging or irritating the tissue underneath [1,11]. Vesicular carriers — liposomes, niosomes, transfersomes and related systems — are one of the more established answers to this problem, and have been used across a wide range of therapeutic classes to raise the amount of drug that actually reaches the systemic circulation via the skin [2,3].

Liposomes in particular are colloidal, spherical vesicles assembled from one or more phospholipid bilayers

* Corresponding author
✉: V. Kavin: kavinkuttyraj583@gmail.com

wrapped around an aqueous compartment [4]. Because the bilayer is chemically similar to the intercellular lipids of the stratum corneum, liposomes tend to associate readily with skin lipids on contact, which has been linked to improved local permeation and a degree of drug retention within the upper skin layers rather than immediate systemic washout [3,5]. They are generally regarded as biocompatible and non-irritant, and their release behaviour can be adjusted through bilayer composition to give a slower, more sustained output over time [6,63]. These properties make liposomes a reasonable starting point for a transdermal carrier system, and they form the basis of the formulation strategy adopted in this work. The specific objective of the present study was to design and characterise a liposome-loaded transdermal patch of demeclocycline hydrochloride — a tetracycline-class antibacterial agent not previously reported, to the authors' knowledge, in this particular liposome-in-patch configuration — with a view to improving its skin permeation and extending its release relative to a plain, non-liposomal patch.

### *Transdermal Drug Delivery Systems*

A transdermal drug delivery system (TDDS) is applied to the skin surface and is designed to release drug at a controlled rate for absorption into the systemic circulation over a defined period, although some systems are intended only for a local, skin-level effect such as anaesthesia or anti-inflammatory action [1,22]. Since Michaels and co-workers first modelled percutaneous drug transport mathematically [7], the technology has been extended to cardiovascular drugs, hormonal therapies, analgesics and, more recently, peptide and protein actives, reflecting a steady broadening of the drug classes considered suitable for this route [21,23].

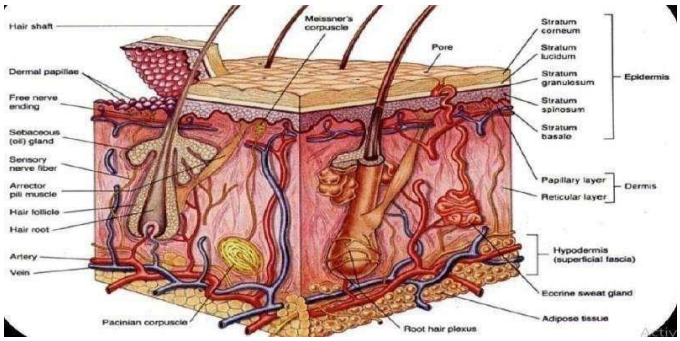


*Figure 1. Cross-sectional anatomy of human skin, showing the epidermis, dermis and hypodermis and their associated structures. The stratum corneum, the outermost epidermal layer, is the principal barrier to drug permeation.*

Anatomically, the skin is arranged in three main strata — the epidermis, with the non-viable stratum corneum as its outer face; the dermis; and the underlying hypodermis [13,14]. A permeant applied to the surface must first cross the stratum corneum before it can reach the viable epidermis and dermis and be picked up by the dermal capillary bed. Three routes are generally described for this crossing: the tortuous intercellular lipid pathway between corneocytes, a direct transcellular path through the corneocytes themselves, and a minor appendageal route via hair follicles and sweat ducts [16,19]. Which route dominates for a given molecule, and how quickly it crosses, depends jointly on the physicochemical make-up of the drug — molecular size, lipophilicity and degree of ionisation — and on skin-side variables such as hydration state, regional thickness and the condition of the barrier [1,12].

### *Liposomes as Skin-Permeation Carriers*

Structurally, a liposome is one or more concentric phospholipid bilayers surrounding an aqueous core (Figure 2). The polar head groups of the phospholipid orient outward, into the surrounding water phase and the internal aqueous compartment, while the non-polar acyl tails associate within the bilayer interior. This arrangement gives the vesicle two distinct compartments — an aqueous core for hydrophilic drugs and a lipid bilayer for lipophilic ones — which is part of why liposomes have been applied to such a broad range of drug molecules in the literature [4,57,63].

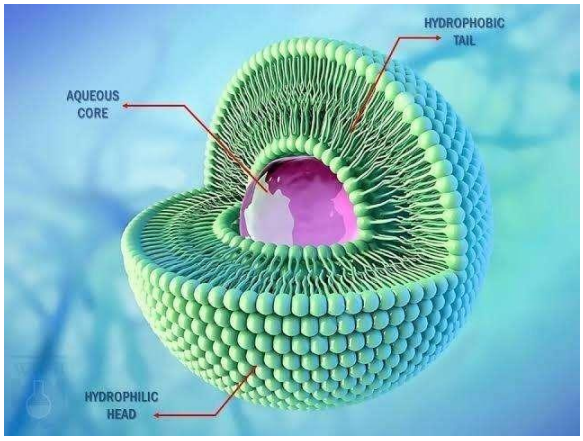


*Figure 2. Schematic structure of a liposome, showing the hydrophilic head groups, hydrophobic tails and the aqueous core in which a hydrophilic drug such as demeclocycline HCl can be entrapped.*

Several mechanisms have been proposed for how liposomes assist skin permeation: they may fluidise or partially disorganise stratum corneum lipids on contact, weakening the barrier locally; they may act as a slow-releasing depot lodged within the upper skin layers; or they may simply raise the effective drug concentration at the skin surface by holding it there longer than a plain solution would [3,5,59]. Cholesterol is almost always co-formulated with the phospholipid for a practical reason — it inserts into the bilayer and reduces its fluidity, which lowers passive leakage of the entrapped drug and gives the vesicle better mechanical stability during storage and handling [57,68]. This stabilising role of cholesterol is one

of the reasons it was retained as a factorial variable in the present optimisation study.

### *Structure of a Transdermal Patch*

Irrespective of drug or carrier, most transdermal patches share a common set of functional layers: an outer backing layer that is impermeable and shields the formulation from the environment, a drug reservoir or drug-in-matrix layer that holds the dose, an adhesive layer that maintains skin contact, and, in reservoir-type designs, a rate-controlling membrane positioned between the reservoir and the skin (Figure 3) [22,23]. On this basis, patches are usually grouped into reservoir systems, single- or multi-layer drug-in-adhesive systems, and matrix systems in which drug is dispersed directly through a polymer film without a separate membrane [23,25]. The present formulation follows the matrix approach: the liposomal dispersion is blended directly into an HPMC/PVA film rather than held behind a separate membrane, which simplifies manufacture while still allowing the liposomes themselves to moderate the release rate.

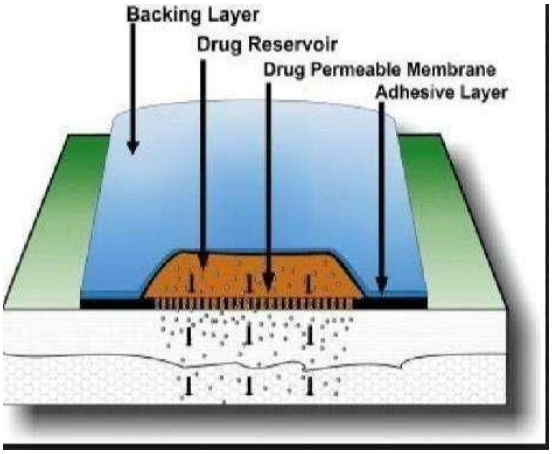


*Figure 3. General architecture of a transdermal drug delivery system, showing the backing layer, drug reservoir, rate-controlling membrane and adhesive layer.*

Taken together, the liposomal carrier and the matrix patch format address complementary parts of the delivery problem — one improves how readily the drug moves across the stratum corneum, the other controls how the dose is presented to the skin over time — and combining them was the central design choice of this study. The rationale, aim and specific objectives that followed from this reasoning are set out below.

## Materials and Methods

### *Drug and Excipients*

Demeclocycline hydrochloride — a tetracycline-class antibacterial with molecular formula C21H21ClN2O8 and a molecular weight of approximately 464.9 g/mol — was selected as the model drug for this work. It presents as a yellow crystalline powder that is only slightly soluble in plain water but dissolves readily in dilute acid or alkali, and it exerts its antibacterial action by binding the bacterial 30S ribosomal subunit and blocking attachment of aminoacyl-tRNA, thereby halting protein synthesis [58]. Soya-derived phosphatidylcholine supplied the bilayer-forming lipid, cholesterol was included as a membrane-stabilising co-lipid [57,68], HPMC K100 served as the principal film-forming polymer, PVA as a secondary support polymer, PEG 400 as plasticiser, and propylene glycol as a chemical permeation enhancer. The full list of materials, their functional role, the quantity used per batch, and their commercial source is set out in Table 1.

**Table 1. Materials used in the formulation of the demeclocycline-loaded liposomal transdermal patch (quantities given per batch of 10 patches).**

| S.No | Material | Role | Quantity | Source |
|---|---|---|---|---|
| 1 | Demeclocycline HCl | Active drug | 100 mg | Apex Pharmaceutics |
| 2 | Phosphatidylcholine | Liposome-forming lipid | 200 mg | Haneil Soyatech Pvt. Ltd. |
| 3 | Cholesterol | Membrane stabiliser | 50 mg | Sigma-Aldrich, India |
| 4 | Chloroform | Solvent | 10 mL | Qualigens |
| 5 | Methanol | Co-solvent | 5 mL | Qualigens |
| 6 | HPMC K100 | Film-forming polymer | 1 g | Fourts India Laboratories |
| 7 | PVA | Patch support polymer | 500 mg | Lopa Pharmaceutics |
| 8 | PEG 400 | Plasticiser | 0.5 mL | Lopa Pharmaceutics |
| 9 | Propylene glycol | Permeation enhancer | 0.5 mL | Lopa Pharmaceutics |
| 10 | Distilled water | Hydration medium | 20 mL | — |

### *Preparation of Demeclocycline-Loaded Liposomes*

Liposomal vesicles were generated by the thin-film hydration technique, the same general approach used in most of the comparable liposome-in-patch systems reported for other actives [63,64,67]. Phosphatidylcholine (200 mg) and cholesterol (50 mg) were co-dissolved in a chloroform:methanol mixture (2:1 v/v) within a round-bottom flask, and the organic solvent was subsequently stripped off under reduced pressure on a rotary evaporator held at 40–45 °C. This step leaves a thin, visually uniform lipid film coating the inner glass wall. Hydrating this film with 20 mL of distilled water carrying 100 mg of dissolved demeclocycline HCl, under gentle mechanical agitation, allows multilamellar vesicles to self-assemble spontaneously around the aqueous drug solution. A brief sonication step was then applied to bring

vesicle size down and narrow the resulting size distribution ahead of patch fabrication.

### *Fabrication of the Transdermal Patch by Solvent Casting*

The liposomal dispersion was worked into a polymer matrix using the solvent-casting technique, following the same broad procedure widely reported for HPMC/PVA-based matrix patches [27,34,38]. HPMC K100 (1 g) was dissolved in 10 mL distilled water, and PVA (500 mg) was separately dissolved in 10 mL of hot water; the two polymer solutions were then combined into one. PEG 400 (0.5 mL) and propylene glycol (0.5 mL) were introduced as plasticiser and permeation enhancer respectively, and the liposomal suspension was added slowly under continuous stirring (30 minutes) to yield a homogeneous casting dope. The mixture was cast into a glass Petri dish and left to dry at ambient temperature for 24 hours; the resulting film was then peeled away and cut into uniform 2 cm × 2 cm patches for downstream evaluation.

### *Experimental Design and Optimisation*

A $3^2$ full factorial design was used to study the influence of formulation variables on patch performance, with phosphatidylcholine (X1), cholesterol (X2) and HPMC K100 (X3) as independent variables, each set at a low, medium and high level (Table 2). Entrapment efficiency (Y1), in-vitro drug release (Y2) and folding endurance (Y3) were taken as the dependent responses. Nine formulations (F1–F9) were prepared according to the design matrix shown in Table 3.

**Table 2. Independent variables and their levels used in the $3^2$ factorial design.**

| Factor | Variable | Low level (−1) | Medium level (0) | High level (+1) |
|---|---|---|---|---|
| X1 | Phosphatidylcholine (mg) | 150 | 200 | 250 |
| X2 | Cholesterol (mg) | 30 | 50 | 70 |
| X3 | HPMC K100 (mg) | 800 | 1000 | 1200 |

Response data for each formulation were fitted to a second-order polynomial of the general form $Y = b0 + b1X1 + b2X2 + b12X1X2 + b11X1^2 + b22X2^2$, where b0 is the intercept, b1 and b2 are the main-effect coefficients, b12 the interaction coefficient, and b11, b22 the quadratic coefficients describing curvature in the response. The significance of each model term was assessed by analysis of variance (ANOVA), taking $p < 0.05$ as the threshold for statistical significance, and model adequacy was checked using $R^2$, adjusted $R^2$, predicted $R^2$ and adequate precision. Response surface and contour plots of phosphatidylcholine (X1) and cholesterol (X2) against each response were used to visualise these relationships, and the formulation with the highest overall desirability — balancing maximum entrapment efficiency, maximum drug release and maximum folding endurance — was selected as the optimised batch for further study.

**Table 3. Formulation design matrix (F1–F9) generated from the $3^2$ factorial design.**

| Formulation | X1: Phosphatidylcholine (mg) | X2: Cholesterol (mg) | X3: HPMC K100 (mg) |
|---|---|---|---|
| F1 | 150 | 30 | 800 |
| F2 | 150 | 50 | 1000 |
| F3 | 150 | 70 | 1200 |
| F4 | 200 | 30 | 800 |
| F5 | 200 | 50 | 1200 |
| F6 | 200 | 70 | 800 |
| F7 | 250 | 30 | 1200 |
| F8 | 250 | 50 | 800 |
| F9 | 250 | 70 | 1000 |

### *Evaluation Methods*

The prepared liposomes and patches were evaluated using standard pharmaceutical methods,

**Preformulation studies:** physical appearance (colour, odour, taste) was compared against USP specifications; melting point was determined by the capillary tube method; solubility was assessed in water, phosphate buffer (pH 7.4) and acidic buffer (pH 1.2); the octanol–water partition coefficient was determined spectrophotometrically; and derived powder properties (bulk density, tapped density, Carr's index, Hausner ratio) were measured by standard procedures.

**UV spectrophotometry:** a calibration curve was constructed in the 2–10 µg/mL range at the drug's absorption maximum (273 nm) and used for all subsequent quantitative estimations.

**Physical evaluation of patches:** weight variation (digital balance), thickness (digital Vernier calliper at three points), folding endurance (manual repeated folding at one point until failure), flatness (percentage constriction of strips cut from different parts of the patch), and visual appearance (clarity, smoothness, absence of air bubbles/cracks).

**Drug content:** a defined area of patch was dissolved in a suitable solvent, filtered, and analysed by UV spectrophotometry at 273 nm against the calibration curve.

**Mechanical and surface properties:** tensile strength was measured using a tensile testing apparatus, and surface pH was measured with a digital pH meter after the patch was allowed to swell in distilled water for one hour.

**Moisture content and moisture uptake:** patches were dried over activated silica gel (moisture content) or stored at 75% relative humidity over saturated sodium chloride solution (moisture uptake), and the weight change was used to calculate each parameter.

**FTIR spectroscopy:** performed on KBr pellets of the drug over 4000–400 $cm^{-1}$ to confirm functional groups and check for drug–excipient interaction.

**Differential scanning calorimetry (DSC):** used to study the thermal behaviour of the pure drug and the formulated patch, and to look for shifts in characteristic thermal peaks that would indicate incompatibility.

**Scanning electron microscopy (SEM):** gold/gold–palladium-coated samples were examined to assess particle shape, size and surface texture.

***Ex-vivo* permeation study:** carried out using excised goat skin mounted, together with a pre-treated cellophane membrane, on a Franz diffusion cell assembly (Figure 4), with phosphate buffer pH 7.4 as the receptor medium maintained at 37 ± 0.5 °C. Samples were withdrawn hourly over 10 hours, replaced with fresh buffer, and analysed by UV spectrophotometry at 272 nm.

*Figure 4. Franz diffusion cell assembly used for the ex-vivo skin permeation study.*

**Release kinetics:** cumulative release data were fitted to zero-order, first-order, Higuchi and Korsmeyer–Peppas models (Figure 5) to identify the predominant mechanism of drug release.

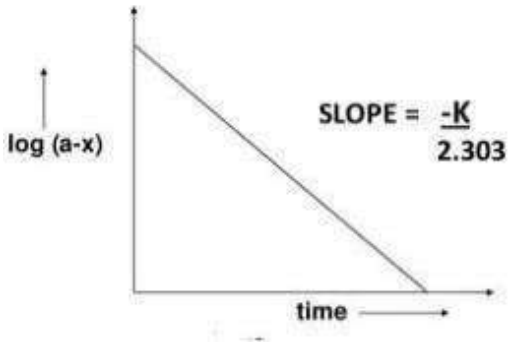


*Figure 5. Representative first-order release plot [log(a–x) versus time] used in the release-kinetic analysis.*

**Antimicrobial activity:** assessed by the agar well diffusion method against E. coli and two Staphylococcus aureus biotypes (SAB1, SAB2), using drug solutions at 10 µg and 20 µg per well with a solvent-only well as control, and measuring the resulting zones of inhibition.

## Results and Discussion

### *Preformulation Studies*

Preformulation work was undertaken as a first step, both to verify the identity and pharmacopoeial-grade purity of the demeclocycline HCl batch on hand and to flag any obvious incompatibility before committing it to formulation, a precaution consistent with standard preformulation practice for transdermal actives [9,12].

**Table 4. Identification test results for demeclocycline HCl.**

| Parameter | Specification | Observation | Inference |
|---|---|---|---|
| Colour | Yellow to pale yellow | Yellow | Complies with USP |
| Odour | Odourless / faint characteristic | Odourless | Complies with USP |
| Appearance | Fine crystalline powder | Fine yellow crystalline powder | Complies with USP |
| Taste | Bitter | Bitter | Complies with USP |

The observed melting point of 208–211 °C matched the literature-reported value of 208–211 °C, further confirming the identity and purity of the drug sample (Table 5).

**Table 5. Melting point determination.**

| Drug | Observed value | Reported value |
|---|---|---|
| Demeclocycline HCl | 208–211 °C | 208–211 °C |

Scanning demeclocycline HCl in phosphate buffer pH 7.4 across the UV range identified a peak absorption at 273

nm, which was then fixed as the analytical wavelength for every subsequent quantitative measurement in the study. A calibration curve built over the 2–10 µg/mL concentration range (Figure 6) was linear across this span, in agreement with Beer–Lambert behaviour, and served as the working reference curve for all drug-content and release calculations reported below.

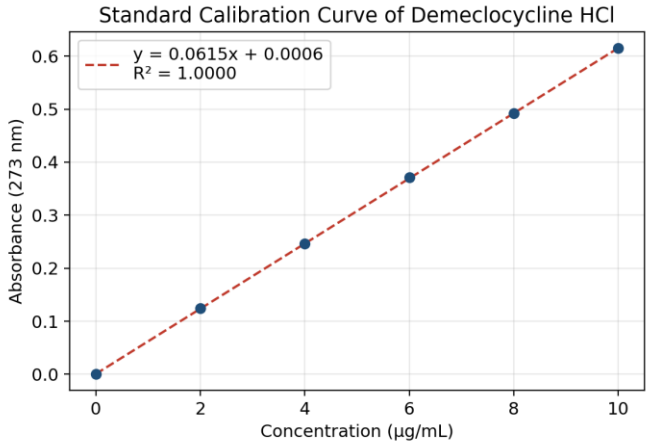


*Figure 6. Standard calibration curve of demeclocycline HCl in phosphate buffer (pH 7.4) at 273 nm.*

Solubility was highest in acidic buffer (pH 1.2, 18 mg/mL), intermediate in distilled water (12 mg/mL), and lowest in phosphate buffer pH 7.4 (8 mg/mL) — a pattern that fits the pH-dependent ionisation typical of a hydrochloride salt [12]. The octanol–water partition coefficient came out at 0.7, sitting within the 1.0–3.0 window generally quoted as acceptable for this compound class, while the derived powder metrics — bulk density 0.42 g/mL, tapped density 0.51 g/mL, Carr's index 16, and a Hausner ratio of 1.21 — together pointed to good, workable powder flow, which is a practical advantage for reproducible batch-to-batch processing [9].

### *Optimisation of the Liposomal Formulation*

Table 6 summarises the entrapment efficiency, in-vitro drug release and folding endurance obtained for the nine factorial-design batches (F1–F9), and Figure 7 presents the entrapment efficiency and drug release data graphically for easier comparison across batches.

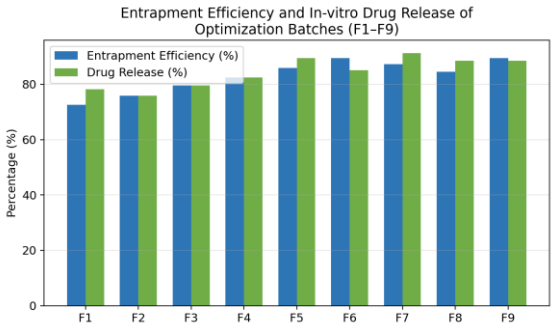


*Figure 7. Entrapment efficiency and in-vitro drug release across the nine optimisation batches (F1–F9).*

**Table 6. Evaluation results of the optimisation batches (F1–F9).**

| Formulation | Entrapment efficiency (%) | Drug release (%) | Folding endurance |
|---|---|---|---|
| F1 | 72.5 ± 0.3 | 78.2 ± 0.5 | 210 ± 2 |
| F2 | 75.8 ± 0.4 | 75.8 ± 0.4 | 225 ± 3 |
| F3 | 79.6 ± 0.5 | 79.6 ± 0.5 | 238 ± 2 |
| F4 | 82.4 ± 0.6 | 82.4 ± 0.6 | 245 ± 3 |
| F5 | 85.9 ± 0.4 | 89.4 ± 0.5 | 258 ± 3 |
| F6 | 89.4 ± 0.5 | 85.1 ± 0.3 | 240 ± 2 |
| F7 | 87.2 ± 0.4 | 91.3 ± 0.5 | 272 ± 3 |
| F8 | 84.5 ± 0.3 | 88.5 ± 0.4 | 255 ± 2 |
| F9 | 89.4 ± 0.5 | 88.5 ± 0.4 | 280 ± 2 |

Entrapment efficiency climbed fairly consistently as the phosphatidylcholine level was raised, which fits the straightforward expectation that more lipid translates into more bilayer material available to enclose the hydrophilic drug [57,63]. Drug release, in turn, tracked HPMC K100 content more closely than it tracked the lipid variables — unsurprising given HPMC's established role as a hydrophilic, swelling matrix former that governs diffusional release once hydrated [23,34]. Folding endurance rose in step with overall polymer loading, which is best read as a mechanical-integrity effect: a denser polymer network simply withstands more repeated flexing before it fails [38,44]. Weighing all three responses together, formulation F7 (250 mg phosphatidylcholine : 30 mg cholesterol : 1200 mg HPMC K100) gave the strongest overall balance and was carried forward as the optimised batch for ex-vivo and microbiological work. A second-order polynomial was fitted to the pooled response data, and ANOVA confirmed the model to be statistically significant ($p < 0.05$), with $R^2$, adjusted $R^2$ and adequate-precision values all within acceptable limits; the associated response-surface and contour plots of phosphatidylcholine against cholesterol were used to visualise the design space and cross-check the F7 selection.

### *Physical and Mechanical Evaluation of the Patches*

Table 7 brings together the weight, thickness, folding endurance, visual appearance and drug content recorded for the nine conventional (non-liposomal) comparator patches, grouped by the three polymer types used — Eudragit, ethyl cellulose and HPMC, each at 1%, 1.5% and 2% w/w — a comparator design broadly similar to the polymer-screening approach used elsewhere in the transdermal-patch literature [27,36,44]. Every batch came out transparent and free of visible surface defects, and drug content rose steadily from F1 through F9, staying

within the range ordinarily accepted for content uniformity in matrix-type patches [23].

**Table 7. Physical evaluation of the fabricated comparator transdermal patches (F1–F9: F1–F3 = Eudragit 1/1.5/2%; F4–F6 = ethyl cellulose 1/1.5/2%; F7–F9 = HPMC 1/1.5/2%).**

| Formulation | Avg. weight (mg) | Thickness (mm) | Folding endurance | Appearance | Drug content (%) |
|---|---|---|---|---|---|
| F1 | 196 ± 0.12 | 0.16 ± 0.02 | 54 ± 1.02 | Transparent | 91.4 |
| F2 | 198 ± 0.18 | 0.17 ± 0.01 | 56 ± 1.10 | Transparent | 92.5 |
| F3 | 201 ± 0.24 | 0.18 ± 0.03 | 58 ± 0.95 | Transparent | 94.6 |
| F4 | 203 ± 0.16 | 0.19 ± 0.02 | 60 ± 1.08 | Transparent | 95.1 |
| F5 | 205 ± 0.21 | 0.20 ± 0.01 | 61 ± 1.14 | Transparent | 96.3 |
| F6 | 207 ± 0.27 | 0.21 ± 0.02 | 63 ± 1.20 | Transparent | 97.0 |
| F7 | 210 ± 0.19 | 0.22 ± 0.03 | 64 ± 1.05 | Transparent | 97.8 |
| F8 | 213 ± 0.23 | 0.23 ± 0.02 | 66 ± 1.12 | Transparent | 98.4 |
| F9 | 216 ± 0.29 | 0.24 ± 0.01 | 68 ± 1.26 | Transparent | 99.2 |

Tensile strength and surface pH results are given in Table 8. Tensile strength rose progressively from E1 through E9, indicating that a heavier polymer loading yields a mechanically tougher film, consistent with the polymer-concentration/tensile-strength relationship reported for other HPMC- and Eudragit-based systems [32,44]. Surface pH, meanwhile, stayed close to neutral throughout (6.2–6.5), a range generally regarded as non-irritant and compatible with prolonged skin contact [31,32].

**Table 8. Tensile strength and surface pH of the fabricated comparator patches.**

| Formulation | Tensile strength (kg/cm²) | Surface pH |
|---|---|---|
| E1 | 2.14 | 6.3 |
| E2 | 2.26 | 6.4 |
| E3 | 2.38 | 6.4 |
| E4 | 2.45 | 6.2 |
| E5 | 2.57 | 6.3 |
| E6 | 2.69 | 6.4 |
| E7 | 2.78 | 6.5 |
| E8 | 2.91 | 6.4 |
| E9 | 3.04 | 6.3 |

Moisture content and moisture uptake (Table 9, Figure 8) both drifted upward as hydrophilic polymer content increased, an unsurprising trend for HPMC-rich films given the polymer's inherent water affinity [23]. Even so, the absolute values stayed low enough throughout to avoid the brittleness or microbial-growth risk that excessive moisture uptake tends to bring, which is a reasonable indication that the patches would hold up physically under normal storage conditions.

**Table 9. Moisture content and moisture uptake capacity of the fabricated comparator patches.**

| Formulation | Moisture content (%) | Moisture uptake (%) |
|---|---|---|
| E1 | 1.80 | 2.10 |
| E2 | 1.92 | 2.20 |
| E3 | 2.04 | 2.40 |
| E4 | 2.12 | 2.50 |
| E5 | 2.24 | 2.70 |
| E6 | 2.48 | 2.80 |
| E7 | 2.57 | 3.04 |
| E8 | 2.69 | 3.18 |
| E9 | 2.72 | 3.36 |

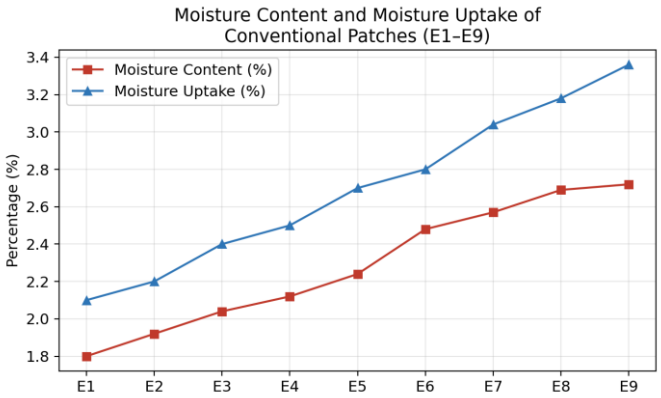


*Figure 8. Moisture content and moisture uptake capacity of the comparator patches (E1–E9).*

### *Compatibility and Surface Morphology Studies*

FTIR scanning of demeclocycline HCl produced the absorption bands expected for its functional groups — a broad O–H stretch, an N–H stretch, and strong C=O and C–O stretching vibrations. None of these bands shifted or disappeared once the drug was incorporated into the patch, which is the usual criterion taken to indicate the absence of any major chemical interaction between drug and excipients [9]. DSC thermograms of the pure drug and the loaded formulation told a consistent story, with no meaningful shift in the drug's characteristic thermal transition after formulation, reinforcing the FTIR-based compatibility conclusion. SEM imaging of the optimised batch was used to check particle shape, size and surface texture, and showed a reasonably uniform, well-dispersed

morphology in keeping with successful vesicle formation and incorporation into the patch matrix.

### *Ex-Vivo Permeation Study*

Table 10 and Figure 9 present the ex-vivo permeation behaviour of the optimised, liposome-loaded patch across excised goat skin — a membrane model commonly used as a practical surrogate for human skin permeation studies [64]. Cumulative release climbed steadily and close to linearly with time, reaching roughly 96% by the 10-hour mark, with no early burst phase evident. A gradual profile of this kind is what the liposomal matrix design was intended to produce: the vesicles appear to moderate how quickly drug becomes available at the skin surface, spreading delivery across the observation window rather than discharging most of the dose in the first hour or two [59,63].

**Table 10. Ex-vivo permeation (cumulative drug release) data for the optimised formulation.**

| Time (h) | Concentration (µg/mL) | Amount released (mg) | Cumulative release (%) |
|---|---|---|---|
| 1 | 1.18 | 0.12 | 12 |
| 2 | 2.26 | 0.23 | 23 |
| 3 | 3.31 | 0.33 | 33 |
| 4 | 4.25 | 0.43 | 43 |
| 5 | 5.18 | 0.52 | 52 |
| 6 | 6.02 | 0.61 | 61 |
| 7 | 6.88 | 0.70 | 70 |
| 8 | 7.72 | 0.79 | 79 |
| 9 | 8.56 | 0.87 | 87 |
| 10 | 9.46 | 0.96 | 96 |

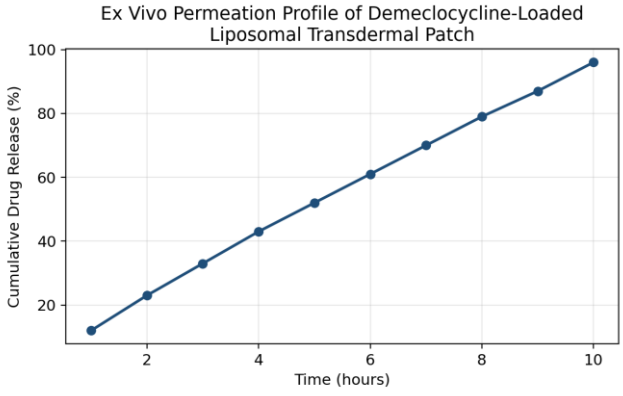


*Figure 9. Ex-vivo cumulative permeation profile of the optimised demeclocycline-loaded liposomal transdermal patch across excised goat skin (Franz diffusion cell, 37 ± 0.5 °C, pH 7.4 receptor medium).*

### *Antimicrobial Activity*

In the agar well diffusion assay, demeclocycline HCl produced clear, measurable zones of inhibition against all three test organisms (E. coli, SAB1 and SAB2), and the zone diameters were consistently larger at the higher drug loading (20 µg versus 10 µg per well) — the expected signature of a concentration-dependent antibacterial effect. The solvent-only control wells showed no inhibition at all, which rules out the vehicle as a contributor and confirms that the activity observed can be attributed specifically to demeclocycline itself. Read alongside the permeation data in the previous section, this is a reasonable indication that drug released from the patch retains its intended antibacterial activity rather than losing potency during formulation.

## Conclusion

The present work set out to design, formulate and evaluate a liposomal transdermal patch of demeclocycline hydrochloride, benchmarking its physicochemical, mechanical and release behaviour against a conventional, non-liposomal patch. Preformulation testing established the identity, purity and acceptable flow characteristics of the drug substance ahead of formulation. Applying a $3^2$ factorial design to phosphatidylcholine, cholesterol and HPMC K100 made it possible to map how each variable, and their combinations, influenced entrapment efficiency, drug release and folding endurance, and this systematic screen pointed to F7 as the batch with the strongest all-round performance. FTIR and DSC data argued against any significant drug–excipient interaction, supporting the chemical and thermal stability of the formulation, and SEM confirmed a reasonably uniform surface morphology. The optimised patch also performed well on the more routine physical checks — consistent weight, thickness and drug content, adequate mechanical strength, a near-neutral surface pH, and moisture content/uptake values low enough to suggest reasonable storage stability.

Ex-vivo testing across excised goat skin produced a steady, sustained permeation profile — close to 96% cumulative release over 10 hours — and agar well diffusion assays confirmed that the drug delivered from the patch retained concentration-dependent antimicrobial activity. Taken as a whole, the data support the view that entrapping demeclocycline HCl in phosphatidylcholine–cholesterol liposomes, and then casting that dispersion into an HPMC/PVA matrix patch, is a workable route to sustained transdermal delivery of this antibiotic. The logical next steps would be in-vivo pharmacokinetic and skin-irritation studies, together with formal stability testing under ICH storage conditions, before the translational potential of this delivery system can be considered fully established.

## Acknowledgement

Authors are thankful to K. M. College of Pharmacy, Madurai, Tamilnadu, India.

## References

1. Gaur, P., et al. (2009). Transdermal drug delivery system,A review. Asian J. Pharm. Clin. Res., 2(1):14-20.
2. Paudel, K.S., et al. (2010). Challenges and opportunities in dermal/transdermal delivery. Ther.Deliv., 1(1): 109-131.
3. El Maghraby, G.M., et al. (2006). Can drug-bearing liposomes penetrate intact skin? J. Pharm. Pharmacol., 58(1): 415-429.
4. Zheng, W.S., et al. (2012). Preparation and quality assessment of itraconazole transfersomes. Int. J. Pharm., 436(1): 291-298.
5. Malakar, J., et al. (2012). Formulation, optimization and evaluation of transferosomal gel for transdermal insulin delivery. Saudi Pharm. J., 20(1): 355-363.
6. Moore, C.L., et al. (1938). Cutaneous absorption of sex hormones. JAMA, 111(1): 14.
7. Michaels, A.S., et al. (1975). Drug permeation through human skin: theory and in vitro experimental measurement. AIChE J., 21(1): 985-996.
8. Sica, D.A. & Grubbs, R. (2005). Transdermal clonidine: therapeutic considerations. J. Clin. Hypertens., 7(9): 558-562.
9. Singh, S., et al. (2012). Preformulation studies of simvastatin for transdermal drug delivery system. Int. Res. J. Pharm., 3(9): 159-161.
10. Fukushima, K., et al. (2011). Two-layered dissolving microneedles for percutaneous delivery of peptide/protein drugs in rats. Pharm. Res., 28(1): 7-21.
11. Pathan, I.B. & Setty, C.M. (2009). Chemical penetration enhancers for transdermal drug delivery system. Trop. J. Pharm. Res., 8(2): 173-179.
12. Igarashi, T., et al. (2007). The appearance of human skin: a survey. Found. Trends Comput. Graph. Vis., 3(1): 1-85.
13. Wilkes, G.L., et al. (1973). The biomechanical properties of skin. CRC Crit. Rev. Bioeng., 1(4): 453-495.
14. Katz, M. & Poulsen, B.J. (1972). Handbook of Experimental Pharmacology (Brodie & Gillette, Eds.). Springer-Verlag, New York.
15. Rushmer, K.F., et al. (1966). The skin. Science, 154(1): 343-348.
16. Patzelt, A., et al. (2008). Hair follicles, their disorders and their opportunities. Drug Discov. Today Dis. Mech., 5(1): e173-e181.
17. Attwood, D. & Florence, A.T. (2012). Skin structure. [Physicochemical Principles of Pharmacy].
18. Schuetz, Y.B., et al. (2005). Emerging strategies for the transdermal delivery of peptide and protein drugs. Expert Opin. Drug Deliv., 2(1): 533-548.
19. Kumar, D., et al. (2011). A review: transdermal drug delivery system: a tool for novel drug delivery system. Int. J. Drug Dev. Res., 3(3): 70-84.
20. Singh, M.C., et al. (2010). Transdermal drug delivery system with major emphasis on transdermal patches: a review. J. Pharm. Res., 3(10): 2537-2543.
21. Aqil, M. (2005). Transdermal drug delivery of labetalol hydrochloride: system development, in vitro, ex vivo and in vivo characterization. Curr. Drug Deliv., 2(2): 125-131.
22. Goswami, D., et al. (2013). Permeation enhancer for TDDS from natural and synthetic sources: a review. J. Biomed. Pharm. Res., 2(1): 19-29.
23. Guyot, M. & Fawaz, F. (2000). Design and in vitro evaluation of adhesive matrix for transdermal delivery of propranolol. Int. J. Pharm., 204(1): 171-182.
24. Patel, R., et al. (2009). Formulation and evaluation of transdermal patch of aceclofenac. Int. J. Drug Deliv., 1(1): 41-51.
25. Mathiowitz, E., Chickering, D.E. & Lehr, C.M. (1999). Bioadhesive Drug Delivery Systems: Fundamentals, Novel Approaches and Development (Vol. 1, pp. 9-44). Marcel Dekker, New York/Basel.
26. Domenic, A. (2015). Transdermal clonidine: therapeutic consideration. J. Clin. Hypertens., 7(9): 558-562.
27. Wahid, A., et al. (2008). Preparation and evaluation of transdermal drug delivery system of etoricoxib using modified chitosan. Indian J. Pharm. Sci., 70(4): 455-460.
28. Bagchi, A., et al. (2010). In-vitro evaluations and skin irritation study of losartan potassium transdermal patches. Iran. J. Pharm. Sci., 6(3): 163-170.
29. Pillai, S., et al. (2011). Effect of polymeric activity on transdermal patches of glipizide. Res. Pharma., 1(2): 1-5.
30. Srivastava, A., et al. (2016). Formulation and evaluation of timolol maleate transdermal patches using various permeation enhancers. Am. J. Adv. Drug Deliv., 4(2): 21-31.
31. Ali, M. & Rajab, N.A. (2014). Preparation and evaluation of domperidone transdermal patches. World J. Pharm. Res., 3(7): 50-78.
32. Aparna, C., et al. (2015). Formulation and evaluation of transdermal patch and gel of nateglinide. Int. J. Pharm. Pharm. Res., 4(2): 1-19.
33. Asija, R., et al. (2015). Formulation and evaluation of transdermal patches of torasemide. Int. J. Adv. Sci. Res., 1(1): 38-44.
34. Kumar, P., et al. (2015). Formulation and evaluation studies on transdermal dosage forms of diclofenac sodium. World J. Pharm. Pharm. Sci., 4(3): 1043-1063.
35. Thejeswi, B., et al. (2015). Formulation and evaluation of transdermal patch containing amphotericin B. Int. J. Nov. Trends Pharm. Sci., 5(4): 123-129.
36. Vinayagam, P., et al. (2015). Formulation and evaluation of gliclazide transdermal drug delivery application. Int. J. ChemTech Res., 8(8): 19-24.
37. Vishvesh, K., et al. (2015). Formulation and evaluation of transdermal patch of cefdinir with various polymers. Pharma Innov. J., 4(6): 74-77.
38. Eisha, G. & Kuldeep, G. (2016). Formulation and evaluation of transdermal patch of acetohexamide. Eur. J. Pharm. Med. Res., 3(7): 233-235.
39. Pokala, M., et al. (2016). Formulation and evaluation of transdermal patches of salbutamol. World J. Pharm. Pharm. Sci., 5(6): 1358-1378.
40. Saleem, M., et al. (2016). Formulation, design and development of a Unani transdermal patch for antiemetic therapy and its pharmaceutical evaluation. Scientifica, 10(1): 1-5.
41. Surender, V., et al. (2016). Formulation, evaluation and optimization of transdermal patches of losartan potassium. World J. Pharm. Sci., 4(5): 277-284.
42. Afrah, S. & Ratnamala, K.V. (2017). Formulation and evaluation of naproxen sodium transdermal patch using natural polymers. Int. J. Pharm. Pharm. Res., 11(1): 161-176.
43. Akhlaq, M., et al. (2017). Design, formulation and evaluation of transdermal patch of propranolol using chamomile essential oil as permeation enhancer: in vitro/in vivo. Polym. Sci., 3(4): 66-71.
44. Cherikuri, S., et al. (2017). Formulation and evaluation of transdermal drug delivery of topiramate. Int. J. Pharm. Investig., 7(1): 10-17.
45. Suksaeree, J., et al. (2017). Formulation, characterization, and in vitro evaluation of transdermal patches for inhibiting crystallization of mefenamic acid. J. Drug Deliv. Sci. Technol.
46. Akram, M., et al. (2018). Formulation, design and development of matrix diffusion controlled transdermal delivery of glimepiride. Drug Des. Devel. Ther., 12(1): 349-364.
47. Kumar, M., et al. (2018). Stable liposome in cosmetic platform for transdermal folic acid delivery for fortification and treatment of micronutrient deficiencies. Sci. Rep., 8(1): 1-12.
48. Kumar, R., et al. (2014). Formulation and evaluation of oleanolic acid loaded transdermal patch. Int. J. Curr. Trends Sci. Technol., 8(3): 20196-20204.

49. Peddapalli, H., et al. (2018). Formulation and evaluation of transdermal patches for antianxiety drug. Asian J. Pharm., 12(2): 127-137.
50. Rahman, S. & Sharma, N. (2018). Formulation and evaluation of matrix transdermal patch of glibenclamide. J. Drug Deliv. Ther., 8(5): 366-371.
51. Renuka, D., et al. (2018). Development and evaluation of transdermal patches with Cissus quadrangularis plant extract. Int. J. Life Sci. Pharma Res., 8(2): 31-34.
52. Sudhakaran, C.K., et al. (2016). A comparison study of liposomes, transfersomes and ethosomes bearing lamivudine. Int. J. Pharm. Sci. Res., 7(10): 4214-4221.
53. MOVA Pharmaceutical Corporation. (2007). Declomycin (demeclocycline hydrochloride) tablets: prescribing information. Manati, Puerto Rico: Glades Pharmaceuticals, LLC.
54. Adhyapak, A.A. & Desai, B.G. (2016). Formulation and evaluation of liposomal transdermal patch for targeted drug delivery of tamoxifen citrate for breast cancer. J. Adv. Pharm. Technol. Res., 7(3): 95-101. doi:10.4103/2231-4040.184594.
55. Mahdiyyah, A.A., Diyah, N.W. & Hendradi, E. (2022). Transdermal patches: a review of a new drug delivery system approach. Int. J. Med. Rev. Case Rep., 6(9): 25-31.
56. Taware, A.D., Thorat, S.S., Waikar, D.M. & Wayal, S.S. (2023). Formulation and evaluation of transdermal patch. Int. J. Pharm. Res. Appl., 8(3): 2454-2464.
57. Chattopadhyay, B., Jain, A.K. & Jain, U.K. (2024). Development and optimization of lamotrigine-containing liposomal transdermal patches. J. Drug Deliv. Ther., 14(5): 130-136.
58. Duangjit, S., et al. (2011). Characterization and in vitro skin permeation of meloxicam-loaded liposomes versus transfersomes. J. Drug Deliv., 1-9.
59. Nave, G., et al. (2011). Formulation and in vitro, ex vivo and in vivo evaluation of elastic liposomes for transdermal delivery of ketorolac tromethamine. Pharmaceutics, 3(1): 954-970.
60. Sharma, S., et al. (2011). Preparation, characterization, in vitro and in vivo evaluation of elastic liposomal formulation of lovastatin. J. Pharm. Res., 4(11): 4074-4078.
61. Taghizadeh, S. & Bajgholi, S. (2011). A new liposomal drug in adhesive patch for transdermal delivery of sodium diclofenac. J. Biomater. Nanobiotechnol., 2(1): 576-581.
62. Kumar, R., et al. (2012). Formulation and evaluation of elastic liposomes of clotrimazole. Int. J. Drug Dev. Res., 4(3): 348-355.
63. Manvir, A., et al. (2012). Elastic liposome mediated transdermal delivery of an antihypertensive agent: nifedipine. J. Drug Deliv. Ther., 2(5): 55-60.
64. Wasankar, S.R., et al. (2012). Formulation and development of liposomal gel for topical drug delivery system. Int. J. Pharm. Sci. Res., 3(11): 4461-4474.
65. Moghimipour, E., et al. (2013). Formulation and in vitro evaluation of topical liposomal gel of triamcinolone acetonide. Res. J. Pharm. Biol. Chem. Sci., 4(1): 101-107.
66. Umalkar, D.G. & Rajesh, K.S. (2013). Formulation and evaluation of liposomal gel for treatment of psoriasis. Int. J. Pharm. Biol. Sci., 4(4): 22-32.
67. Manjula, D., et al. (2014). Topical delivery of fenoprofen proliposomes: preparation, evaluation and in vitro release. Int. J. Pharm. Sci. Invent., 3(8): 6-12.
68. Szura, D., et al. (2014). The impact of liposomes on transdermal permeation of naproxen. Acta Pol. Pharm. Drug Res., 71(1): 145-151.
69. Tiwari, G., Tiwari, R., Sriwastawa, B., et al. (2012). Drug delivery systems: an updated review. Int. J. Pharm. Investig., 2(1).
70. Nwobodo, N.N., Adamude, F.A., Dingwoke, E.J. & Ubhenin, A. (2019). Formulation and evaluation of elastic liposomes of decitabine prepared by rotary evaporation method. Univ. J. Pharm. Res., 4(3): 1-5.
71. Farooque, F., Wasi, M. & Mughees, M.M. (2021). Liposomes as drug delivery system: an updated review. J. Drug Deliv. Ther.
72. Padole, D.U., Pande, S.D., Sawarkar, R.A., et al. (2023). Review on recent advances in liposomal drug delivery system. Int. J. Creat. Res. Thoughts.
73. Maniyar, M.G., Zadbuke, D.M., Chakorkar, S.S. & Mahamuni, R.C. (2024). Liposomes based drug delivery system. Pharm. Reson., 6(2).
74. Chattopadhyay, B., Jain, A.K. & Jain, U.K. (2024). Development and optimization of lamotrigine-containing liposomal transdermal patches. J. Drug Deliv. Ther., 14(5): 130-136.